Vol.2, No.4, Page 391- 402, 2024 https://doi.org/10.59628/jast.v2i4.1145 ISSN 2958-9568 JAST

Sun Publisher

مجلة جامعة صنعاء للعلوم التطبيقية والتكنولوجيا
Sana'a University Journal of Applied Sciences and Technology
https://journals.su.edu.ye/index.php/jast/

Titanium Complex with New Schiff Base 4-(N, N-dimethylaminobenzylidene)-1-phenylsemicarbazide: Synthesis, Thermal, XRD, and Antibacterial properties

Fathi M. Al-Azab[1], Yasmin M. S. Jamil[1*], Nedhal A. A. Al-Selwi[1], Ahmed N. Alhakimi[2,3], Dheya A. Hameed[1], Gamil M. S. Qasem[1,4] and Abuzar Ebead Albadri[3,5]

[1]**Department of Chemistry, Faculty of Science, Sana'a University, Sana'a, Yemen,**
[2]**Department of Chemistry, Faculty of Science, Ibb University, Ibb, Yemen,**
[3]**Department of Chemistry, Faculty of Science, Qassim University, Buraidah 51452, Saudi Arabia,**
[4]**Department of Chemistry, Faculty of Applied Sciences, Thamar University, Yemen,**
[5]**Department of Chemistry, Faculty of Science, University of Khartoum, Sudan.**

*Corresponding author: y.jamil@su.edu.ye

Abstract

4-(N, N-dimethylaminobenzylidene)-1-phenylsemicarbazide Schiff base (SB) was synthesized from 1-phenylsemicarbazide and 4-(N,N-dimethylaminobenzaldehyde). Numerous analytical approaches, such as elemental analysis, ^{1}HNMR, ^{13}CNMR, electronic spectra, and FT-IR spectroscopy were utilized to analyze the newly synthesized Schiff base. The Ti (IV) Schiff base complex was produced, and its electrolytic nature, stability, and octahedral structural properties were determined by elemental, IR, UV-Vis spectral, conductivity, and thermal studies (TGA-DTA). From XRD results, the practical size of Schiff base and its complex were in the nano range with crystallinity structure. To evaluate the antibacterial activity, the free ligand and its complex were assessed in vitro against *Pseudomonas aeruginosa, Escherichia coli, and Staphylococcus aureus*. These results show that the metal complex has stronger antibacterial action than the Schiff base ligand.

Article Info

Keywords:
Schiff base, Ti (IV) complex, Thermal analysis, XRD, Antibacterial Study

Article History:
Received: 24-July-2024,
Revised: 13-August-2024,
Accepted: 18-August-2024,
Available online: 30 August 2024.

1. INTRODUCTION

The Schiff base is a nitrogen analogue of an aldehyde or ketone in which the nitrogen atom is linked to an aryl or alkyl group but not hydrogen when the C=O group is substituted with the C=N group [1, 2]. The azomethine group, whose typical formula is RHC=N-R_1 (where R and R_1 can be heterocyclic, aryl, or alkyl groups), is the essential component of these analogues [3, 4]. These substances are also referred to as anils, imines, or azomethine [5, 6]. The most significant organic compounds with a wide range of uses are Schiff's bases [7], which are widely employed as stabilizers [8], insecticides [9], dyes, polymer industry catalysts [10], stabilizers in many organic reactions, and more [11]. A survey of the literature reveals a work devoted to the synthesis, characterization, and biological activities of many metal complexes of Schiff base from 1-phenylsemicarbazide [12–15]. Similarly, these substances exhibit a range of biological or pharmacological properties, such as anti-inflammatory [16], anti-HIV [17], anti-urea [18], anticholinesterase [19], and others. This paper describes the synthesis and characterization of the Schiff base 4-(N,N-dimethylaminobenzaldehyde)-1-phenylsemicarbazide and it's complex with Ti (IV), a ligand that has been the focus of numerous investigations due to its diverse biological activities.

2. MATERIALS AND METHODS

2.1. Materials

High-purity chemicals were used by the BDH company. These chemicals were 1-phenylsemicarbazide, 4-(N,N-dimethylaminobenzaldehyde), calcium chloride, and Titanium chloride tetrahydrate ($TiCl_4.4H_2O$). The solvents used were of spectroscopic grade.

2.2. Preparation of Schiff base

In an equimolar ratio of 1:1, a solution of 1-phenylsemicarbazide (3 g, 0.02 mol) in 50 ml of warm absolute ethanol was added dropwise to 4-(N,N-dimethylaminobenzaldehyde) (2.98 g, 0.02 mol) in 50 ml of warm absolute ethanol (Scheme 1). For five hours, the mixture was refluxed on a hot plate. A white crystalline solid was the product of the reaction, which was filtered out and dried over anhydrous $CaCl_2$ in a desiccator.

2.3. Preparation of Ti (IV) Schiff base Complex

The Titanium (IV) Complex was prepared by combining metal chloride in 50 ml of absolute ethanol with a well-stirred solution in absolute warm ethanol of Schiff base at stoichiometric ratios (1L:1M) (Scheme 2). After refluxing the mixture for three hours on a hot plate while stirring, it was allowed to cool to room temperature. After filtering and repeatedly washing with diethyl ether, the thin precipitate that separated was dried over anhydrous $CaCl_2$.

2.4. Spectral measurements

At Sana'a University, the compounds infrared spectra were measured in the 200–4000 cm^{-1} range using the (FT/IR-140, Jasco, Japan) equipment. The compounds electronic spectra were measured at Sana'a University using a UV-VIS spectrophotometer (specord200, Analytilk Jena, Germany) in the 200–800 nm range. Using Bruker spectroscopy, the proton NMR spectra were acquired at 25 ℃, 850 MHz and 213 MHz, respectively. The compounds C, H, and N analyses were conducted in Vario EL Fab. CHN Nr. 11042023, at Central Laboratory, Faculty of Science, Cairo University, Egypt. Silver nitrate was used to determine chloride gravimetrically. Thermal analysis techniques and the weight loss method were used to determine the coordinated and uncoordinated water contents gravimetrically.

2.5. Physical Measurements

Using a Jenway conductivity meter model 4510, the molar conductance of 10^{-3} M solution of the Ti complex in DMSO solvent was determined. On recently made solutions, the measurement was made at room temperature. The ligand and its complex melting points in glass capillary tubes were measured in degrees Celsius using the Stuart Scientific electrothermal melting point device. The XRD patterns were obtained using XD-2 (Shimadzu ED-720) powder X-ray diffractometer at a voltage of 35 kV and a current of mA using CuK(α) radiation in the range of $5^o < 2\theta < 70^o$ at 1^o min^{-1} scanning rate and a wavelength 1.54056 A^o, at Yemen Geological Survey and Mineral Resources Board.

2.6. Crystallinity and particle size

From the XRD percentage of crystallinity, XC (%) was calculated based on the integrated peak areas of the principal peaks [20]. The crystallinity of the complexes is calculated relative to the crystallinity of the ligands as a ratio:

$$XC\,(\%) = (A_{complex})/(A_{ligand}) \times\; 100$$

Where Acomplex and Aligand are the areas under the principal peaks of the complex and ligand sample, respectively. X-ray diffraction was also used to determine the average particle size (D) which was estimated by the Scherrer equation [21, 22]:

$$D = K\lambda/\beta\, cos\theta$$

where K is Scherrer constant and equals 0.94, λ is the X-ray wavelength of Cu-Kα radiations (1.5405 A^o), β is full width at half maximum (FWHM) and θ is Bragg diffraction angle in degrees.

2.7. Thermal Analysis

Differential Thermal Analysis (DTA) and Thermogravimetric Analysis (TGA) experiments were conducted by using Shimadzu simultaneous DTA-TG apparatus (DTG-60AH, Japan); the heating rate was 10℃/min, rate in a temperature range of 27-525℃, and Al_2O_3 served as the reference material for the DTG measurements at Micro Analytical Center, Alqasim University.

2.8. Biological Screening

Three bacteria - *Staphylococcus aureus*, *Pseudomonas aeruginosa*, and *Escherichia coli*- were used to test the antibacterial properties of the synthesized Schiff base and its complex. Using the Agar well diffusion method [23], the antibacterial activity was determined. DMSO was utilized as a solvent to make stock solutions with a concentration of 1000 μg/ml. These solutions were then utilized to prepare different concentrations, which included 100, 200, and 300 μg/ml, respectively. The nutrient agar's surface was infected with the microorganisms. The wells and ditches made on the agar plates

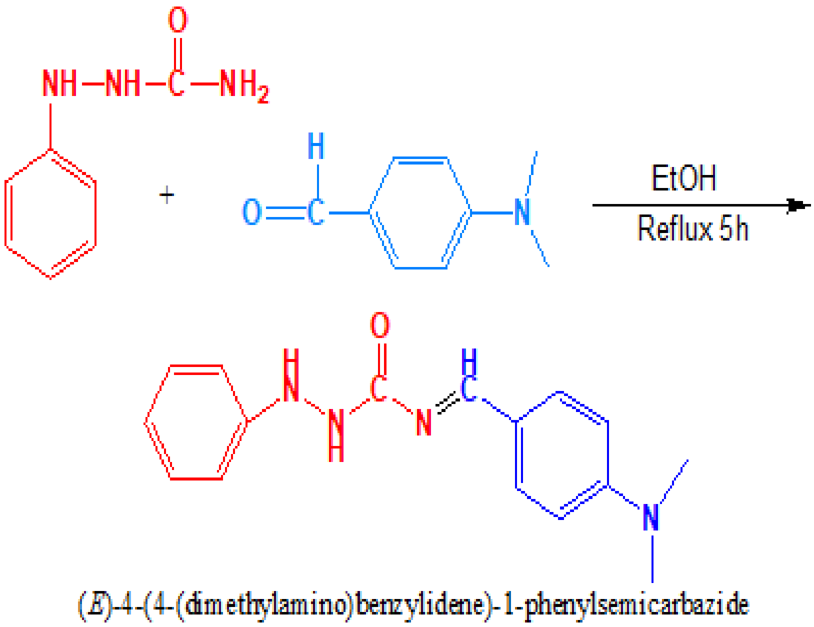

Scheme 1. Synthesis of Schiff base.

Table 1: **Some physical properties and Elemental Analysis of the ligand and its complex**

Compound	Colour (Yield)%	M.P. (C^0)	Λm (Ω^{-1} cm^2 mol^{-1})	F . Wt (g/mole)	Element Analysis Calculated% (Found)		
					C	H	N
SB	White 85.09	202	-	282	68.09 68.01	6.45 6.37	19.87 19.81
$[Ti(SB)Cl_2 (H_2O)_2]Cl_2 . 2H_2O$	Green 79.18	>350	121.22	541	46.12 46.07	2.86 2.84	16.37 16.36

were inoculated with the different concentrations of the compounds. Gentamicin 120 μg/ml was used as a reference substance. All the Petri dishes were put in an incubation period at 37 ℃ for 24 hours. The results were registered by calculating the diameter of the inhibition zone (mm).

3. RESULTS AND DISCUSSION

By condensation of 1-phenylsemicarbazide with 4-(N,N-dimethylaminobenzaldehyde) at a molar ratio of 1:1, the Schiff base was produced. It was found that the ligand ratio of SB with the Ti(IV) was 1:1. Every synthetic compound has a bright colour, is stable, and may be kept for extended periods at room temperature. The Ti(IV) complex of SB has molar conductance value of 121.22 Ω^{-1} cm^2 mol^{-1} in DMSO (1×10^{-3}M). This result indicates that the complex of Schiff base is soluble in water and common organic solvents because it is an electrolyte of type 1:2 [24]. Thermal analysis, elemental analysis, FT-IR, 1HNMR, and 13CNMR, electronic spectra were used to describe the Schiff base and its complex. Some of the physical and analytical details about the Schiff base and its complex are listed in Table 1.

3.1. ^{1}HNMR Spectrum

When interpreting the SB ^{1}HNMR spectrum (Figure 1), several unique peaks can be seen. First, the (s,3H, N-CH^3) amine group was ascribed to the signals at δ(5.976) ppm. The protons in the aromatic ring are responsible for another set of numerous peaks between δ(6.698–7.793) ppm [25]. Here, the pattern suggests a para-substituted phenyl ring with slightly distinct resonant frequencies. Another set of peaks to take into account is located at δ(7.602–7.767) ppm and represents the protons in the carboxamide group. Finally, a singlet signal located at around δ(9.676) ppm suggests the existence of protons connected to the (s, 1H, HC=N) azomethine group [15]. The distinct orientations and chemical surroundings of the protons provide the multiplet and broad nature of the peaks seen in the ^{1}HNMR spectrum, providing crucial information on the structure of the compound.

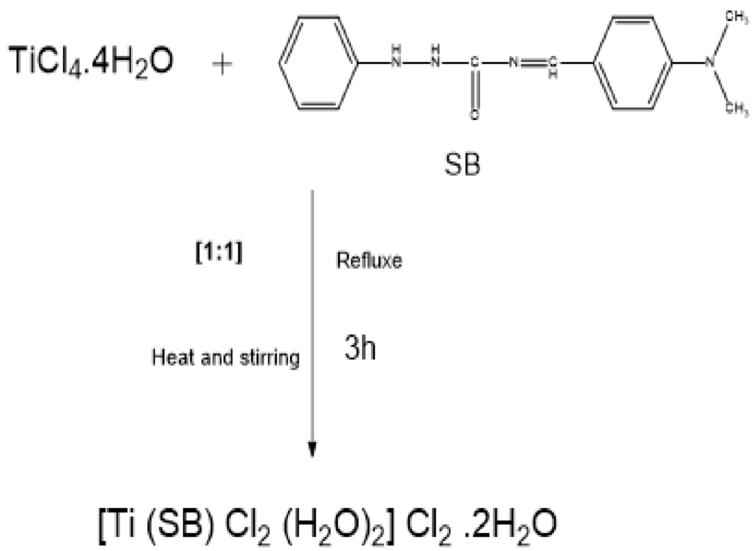

Scheme 2. Synthesis of Ti (IV) complex.

3.2. ^{13}CNMR Spectrum

The ^{13}CNMR spectrum (Figure 2) of the synthesized SB showed peaks at δ(190.33) ppm assigned to (C=O) [26]. Also, the spectrum showed a peak at δ(154.65) ppm that was attributed to azomethine carbon (C=N) [27]. The number of peaks between 111.20, 132.02, 112.63, and 129.44 ppm is attributed to aromatic and 4-aminobenzaldehyde ring carbon in SB, respectively. The carbon of the methyl amine group (N-CH3) appeared at 44.35 ppm in SB [28].

3.3. IR Spectra Studies

The main IR absorption bands of the SB and its complex are summarized in Table 2 and Figure 3. IR spectrum of ligand SB showed bands at 1688 cm-1 and 1600 cm-1 assigned to v(C=O) and v(C=N), respectively [12,13]. The strong bands of v(NH) in this ligand were found at 3335 and 3398 cm-1 [29]. The stretching mode of vibrations of v(-C-N) amide and v(-C-N) amine were observed at 1240 cm-1 and 1200 cm-1, respectively. The bands were noticed at 3040 and 2930 cm-1 that belong to aromatic v(C-H), and aliphatic v(C-H) stretching modes of vibrations, respectively [14]. The IR spectrum of the Ti complex (Figure 3) has been studied by the estimate of its structure. The shift of azomethine vibrations to the lower frequency indicates the coordination of nitrogen with metal ions. New vibrations at 597.74, and 681.89 cm-1 that are not present in the free ligand are attributed to the existence of v(M-N) and v(M-NH), respectively [12]. The broad bands have been seen (2880-3420) cm-1 which correspond to the water molecules in the complex formation [13]. Despite analytical limitations preventing the detection of v(M-Cl) in the IR data.

3.4. The electronic spectra

Three absorption bands at 348, 272 and 300 nm were shown in the electronic spectrum of SB (Figure 4 and Table 3), which are related to the n-π^* and $\pi - \pi^*$ transitions, respectively [12]. These transitions, which move to longer wavelengths (370, 280, and 311) in the case of the Ti complex, have been studied and have confirmed the ligand-to-metal charge transfer (LMCT) and the reverse. For the Ti (IV) complex, LMCT suggests an octahedral structure [30]. The proposed octahedral geometry of the Ti (IV) complex is in Figure 5.

3.5. X-ray diffraction

Figures (6 and 7) represent the XRD patterns for SB and its complex. From these Figures, a remarkable shift of the principal peak toward higher diffraction angles (Table 4) is observed for the complex, suggesting the reduction of the unit cell dimensions and consequently contracting the crystal lattice [12]. In addition, the significant changes in intensities of the main peaks of the SB complex are observed in this figure attributed to the reduction in crystallinity. The crystallinity calculations are based on the ratio of the principal peak area of the complex sample to that of the ligand sample obtaining a relative crystallinity [20]. The results in Table 4 show significant changes in crystallinity between SB and its complex that exhibit low relative crystallinity (15.114%). In literature, the range between 1-100 nm is reported to be nanoparticle size [31]. So the particle size of the Schiff base and its complex obtained from XRD shows effects on their

Table 2: IR absorption bands of the Schiff base and its complex

Compound	M-NH	C=N	C=O	C=C	C-N Amide	C-N Amine	C=C Aliph	M-N M-NH
SB	3335 3398	1600	1688	1495	1240	1200	1645	-
$[Ti(SB)Cl_2(H_2O)_2]Cl_2 \cdot 2H_2O$	3020 3250	1535	1636	1495	1248	1190	1637	597 681

Table 3: Spectral properties of the prepared compounds

Compound	λ_{max} (nm)	Assignments	Suggested Structure
SB	348	(n-π^*, C=O)	………
	272	(n –π^*, C=N)	
	300	(π – π^*, aromatic ring)	
	370	(n-π^*, C=O)	Octahedral
	280	(n –π^*, C=N)	
	311	(π –π^*, aromatic ring)	

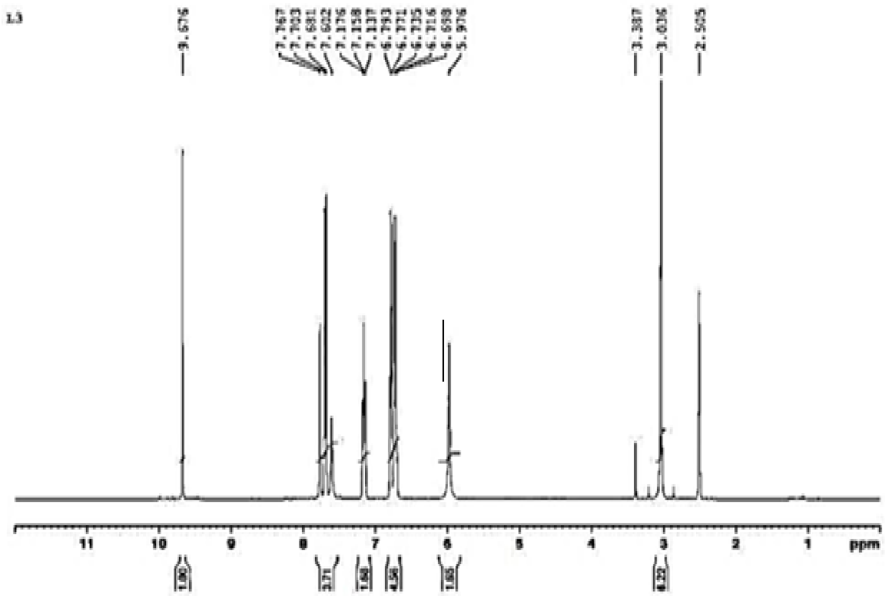

Figure 1. ^{1}H NMR spectrum of SB.

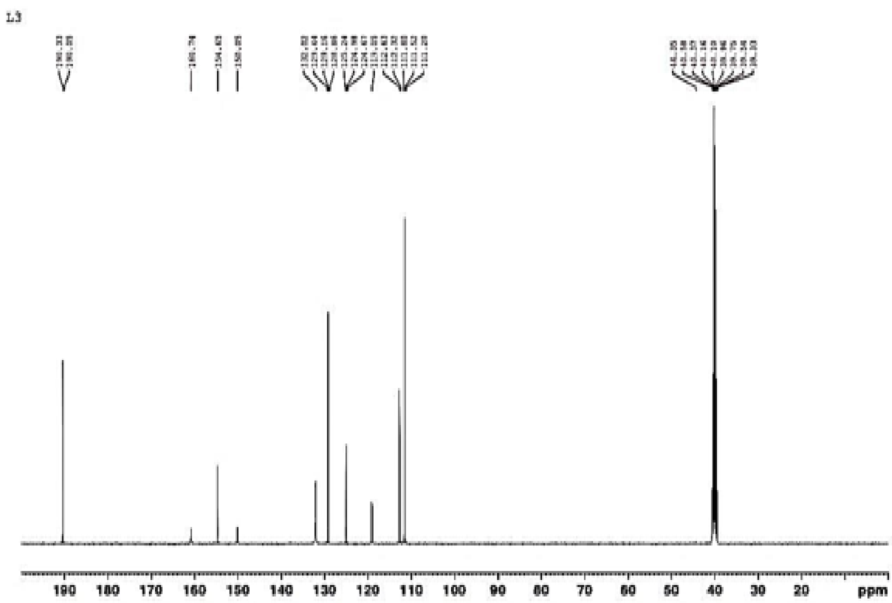

Figure 2. ^{13}C NMR spectrum of (DPHC).

nanoparticle size (3.532 and 5.796 nm)

3.6. Thermal Analysis

The TG degradation curve of [Ti(SB)$Cl_2(H_2O)_2$]Cl_2.2H_2O (Figure 8) reveals five decomposition stages at 30-116, 116-240, 240-322, 322-427 and 427-533℃ as shown in Scheme 3 [32]. The elimination of two uncoordinated water molecules endothermically occurs as a broad peak in the first step (cal. 6.654%, found at 7.023%) with T_{DTG} and T_{dta} at 80℃ and 78℃, respectively. The removal of coordinated water molecules (Cal. 6.654%, found 7.135%) takes place in the second step with T_{DTG} at 215℃ and exothermic T_{dta} at 213℃. The third step corresponds to the loss of the two outer chloride atoms (Cal. 12.933%, found 12.990%) as the T_{DTG} (322℃) and exothermic T_{dta} (228℃) peaks. The fourth step at T_{DTG} 368℃ was assigned to the release of one chloride atom in the complex (Cal. 6.562, found 6.584%). The fifth step of T_{DTG} at 510℃ is assumed to correspond elimination of one chloride atom in the complex (Cal. 6.562%, found at 6.584%). The residue at the end of the decomposition reaction is (- $C_{16}H_{16}N_4Ti$) (Cal. 60.635%, found 59.673%).

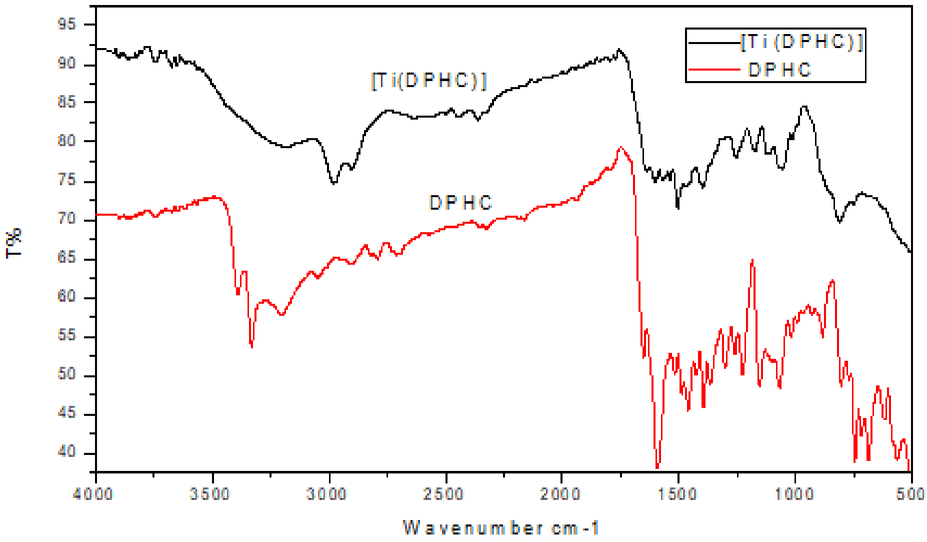

Figure 3. IR Spectra of SB and its Ti (IV) complex.

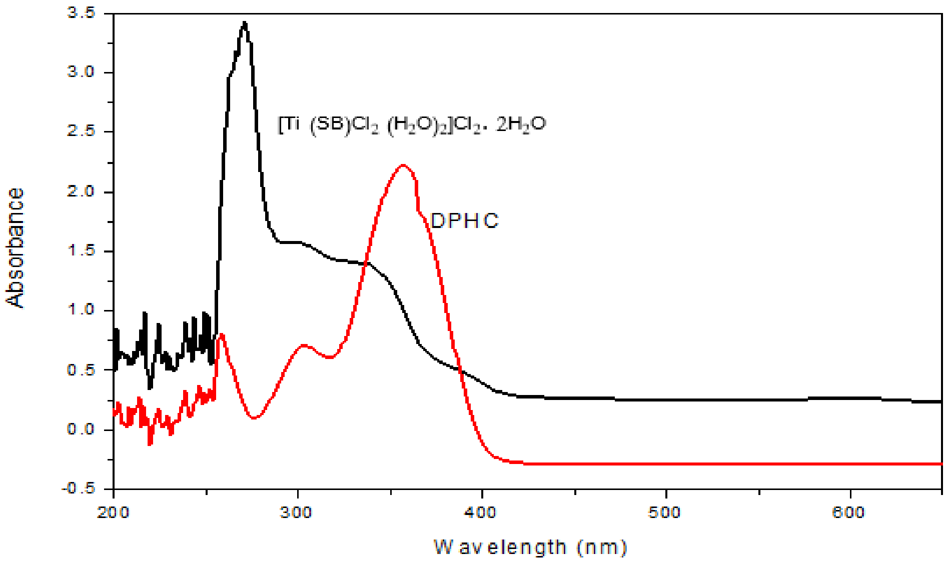

Figure 4. Electronic Spectra of Schiff base and its Ti (IV) complex

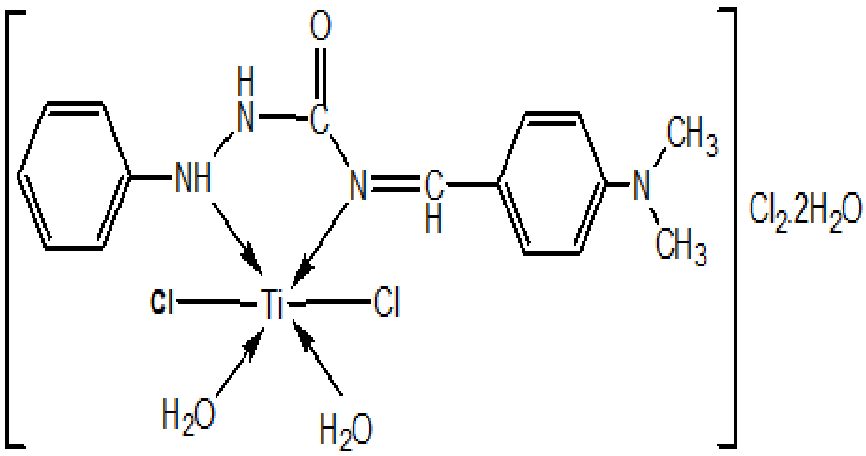

Figure 5. The proposed octahedral geometry of Ti (IV) complex.

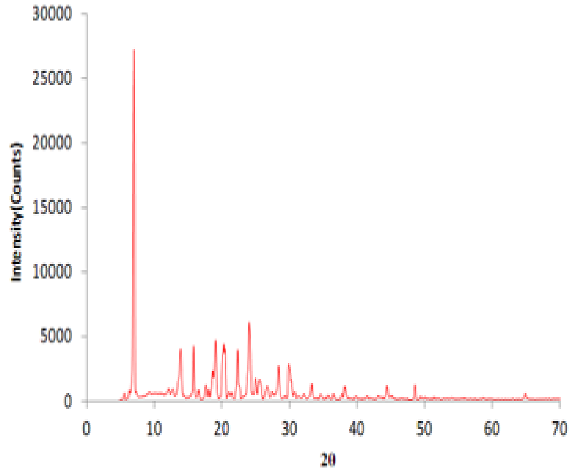

Figure 6. XRD pattern of SB.

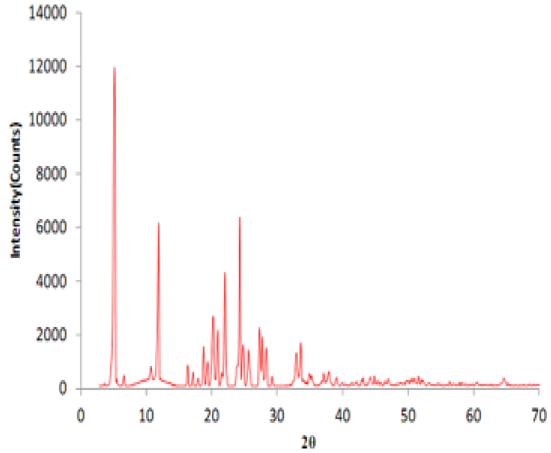

Figure 7. XRD pattern of Ti (IV) complex.

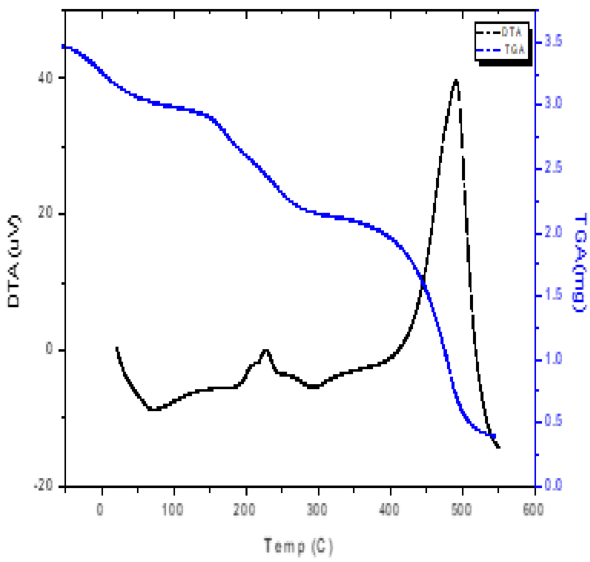

Figure 8. Curves of TGA and DTA of Ti (IV) complex.

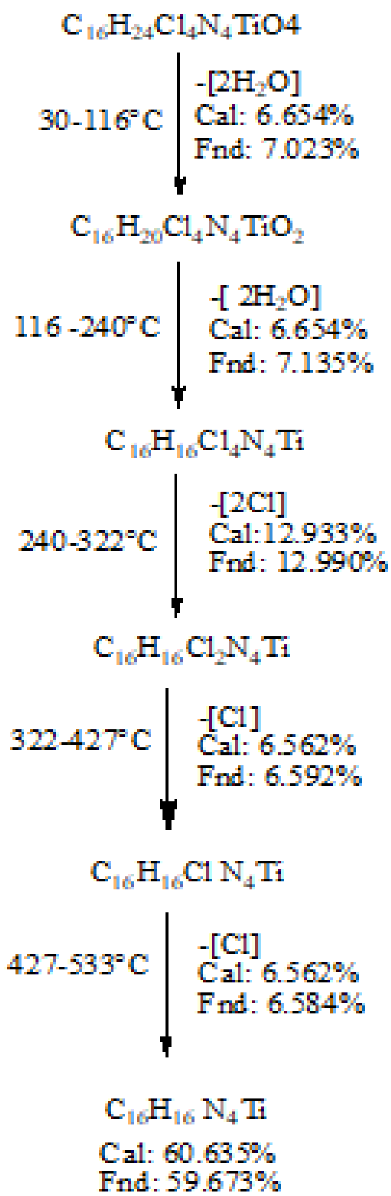

Scheme 3. The proposed Degradation of Ti(IV) complex.

Table 4: **XRD spectra data of the principal values of intensity of the SB and its complex**

Compound	2θ	β	D (nm)	Mean D	X_C (%)
SB	8.151 15.130 18.095 20.300 21.905 23.570	0.229 0.539 0.231 0.969 0.832 0.590	6.339 2.710 6.348 1.518 1.772 2.507	3.532	100
$[Ti(SB)Cl_2(H_2O)_2]Cl_2.2H_2O$	6.390 14.060 24.244 26.520	0.360 0.214 0.249 0.233	4.029 6.820 5.949 6.387	5.796	15.114%

Table 5: Characteristic parameters of thermal decomposition (10°C min^{-1}) for Ti (VI) complex

Compound	Step	TGA				DTA		*Reaction*
		Δ m % (calc.) found	T_i/C°	T_f/C°	T_{DTG}	T_{dta}	Heat	
$[Ti(SB)Cl_2(H_2O)_2]Cl_2.2H_2O$	1	6.654 7.023	30	116	80	78	endo	$-2H_2O$
	2	6.654 7.135	116	240	215	213	exo	$-2H_2O$
	3	12.933 12.990	240	322	246	228	exo	- 2 Cl
	4	6.562 6.584	332	427	368	370	endo	- Cl
	5	6.562 6.584	427	533	510	491	exo	- Cl
Final residue (- $C_{16}H_{16}N_4Ti$) :(60.635%) – (59.673%)								

3.7. Antibacterial Studies

Using the well diffusion method [23], the ligand and its Ti(VI) complex were tested for antibacterial activity against three different species of bacteria: Pseudomonas aeruginosa, Escherichia coli, and Staphylococcus aureus (Figures 9 and 10). They were classified as moderately active and highly active based on the diameter of the zone of inhibition (mm), which was used to measure the antibacterial activity. Table 6 provides a summary of the results obtained.

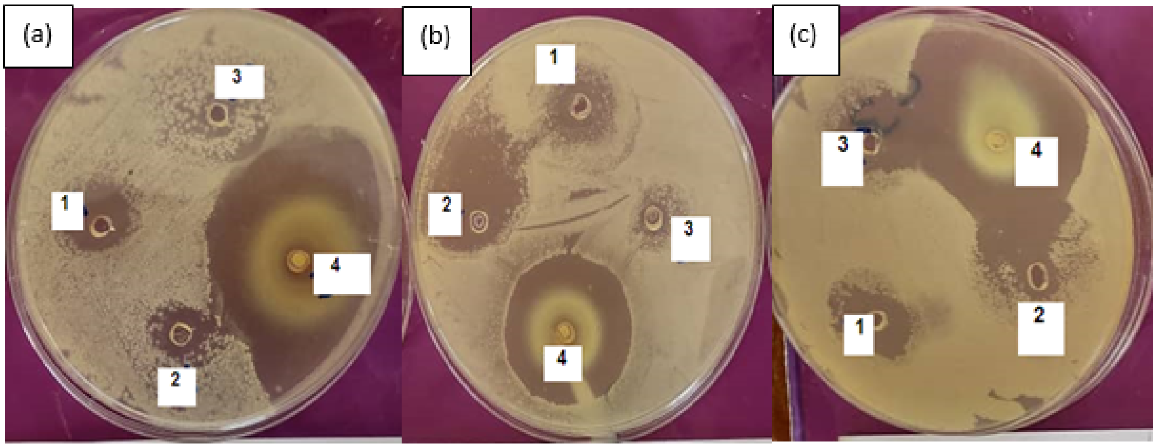

Figure 9. zone of inhibition of SB versus (a) Staphylococcus aureus, (b) Pseudomonas aeruginosa and (c) Escherichia coli [(1) 100 μg/ml, (2) 200 μg/ml, (3) 300 μg/ml, (4) Gentamicin 120 μg/ml].

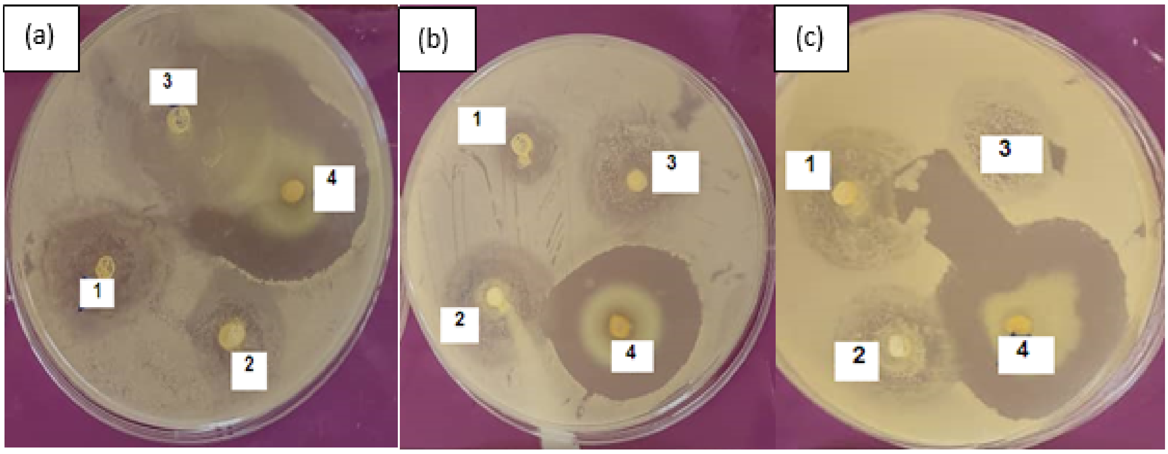

Figure 10. zone of inhibition of Ti (VI) complex versus (a) Staphylococcus aureus, (b) Pseudomonas aeruginosa and (c) Escherichia coli [(1) 100 μg/ml, (2) 200 μg/ml, (3) 300 μg/ml, (4) Gentamicin 120 μg/ml].

Table 6: The effect of the SB and its complex on the growth of Bacteria (Zone of inhibition in mm)

Compound	Concentration µg/ml	*Staphylococcus aureus*	*Pseudomonas aeruginosa*	*Escherichia coli*
SB	100	10	8	12
	200	15	12	14
	300	17	15	18
$[Ti(SB)Cl_2(H_2O)_2]Cl_2.2H_2O$	100	12	10	12
	200	16	12	15
	300	18	16	20
Gentamicin	120 µg/ml	35	30	34

4. CONCLUSION

In the current work, we produced a novel Schiff base, 4-(N, N-dimethylaminobenzylidene)-1-phenylsemicarbazide, together with its Ti (IV) complex. These substances were described by using various physicochemical and spectrum techniques. The results of the UV-Vis and IR studies indicated that the metal. Complex formed the octahedral geometry because of the (NH) and (C=N) nitrogen in the SB. The XRD patterns of the free ligand and its complex exhibited notable changes, and the composition of the crystal was revealed along with them. The results on antibacterial activity indicated that the complex exhibited better inhibitory action compared to the ligand.

REFERENCES

[1] S. Bhandarkar, P. Pathare, and B. Khobragade, "New nickel (ii), copper (ii) and cobalt (ii) complexes based salicyaldehyde schiff base: Synthesis, characterisation, and antiviral activity," *Mater. Today: Proc.*, vol. 92, pp. 807–816, 2023. DOI: 10.1016/j.matpr.2023.04.381.

[2] J. Zhao and G. Cui, "Study on adsorption and complexation behaviour of thiourea on the copper surface," *Int. J. Electrochem. Sci.*, vol. 6, no. 9, pp. 4048–4058, 2011. DOI: 10.1016/s1452-3981(23)18309-x.

[3] A. Allouch, I. El Hassan, and M. Bouchkara, "Synthesis and characterization of complexes of some transition metals with two bifunctional thiourea derivatives," *Chem. Sci. Trans.*, vol. 7, no. 2, pp. 290–296, 2018. DOI: 10.7598/cst2018.1476.

[4] M. Emami Khansari, K. Wallace, and M. Hossain, "Synthesis and anion recognition studies of a dipodal thiourea-based sensor for anions," *Tetrahedron Lett.*, vol. 55, no. 2, pp. 438–440, 2014. DOI: 10.1016/j.tetlet.2013.11.050.

[5] A. Abu-Yamin, M. Abduh, S. Saghir, and N. Al-Gabri, "Synthesis, characterization and biological activities of new schiff base compound and its lanthanide complexes," *Pharmaceuticals*, p. 454, 2022. DOI: 10.3390/ph15040454.

[6] H. Afridi *et al.*, "Synthesis and investigation of the analgesic potential of enantiomerically pure schiff bases: A mechanistic approach," *Molecules*, vol. 27, no. 16, p. 5206, 2022. DOI: 10.3390/molecules27165206.

[7] T. Ghali and J. Tomma, "Synthesis and characterization of indazol-3-one and thioxo pyrimidines derivatives from mono and twin chalcones," *Iraqi J. Sci.*, vol. 58, no. 4C, pp. 2266–2277, 2017. [Online]. Available: https://ijs.uobaghdad.edu.iq/index.php/eijs/article/view/29.

[8] O. El-Gammal, F. Mohamed, G. Rezk, and A. El-Bindary, "Structural characterization and biological activity of new metal complexes based on schiff base," *J. Mol. Liq.*, vol. 330, p. 115 522, 2021. DOI: 10.1016/j.molliq.2021.115522.

[9] Filipovietal, "Biological activity of two isomeric n-hetero aromatic selenosemicarbazone and their metal complexes," *Monatsh Chem.*, vol. 109, pp. 145–1089, 2014. DOI: 10.1007/s00706-014-1197-6. [Online]. Available: http://dx.doi.org/10.1007/s00706-014-1197-6.

[10] D. Shobha and S. Borhade, "Synthesis, structure, spectroscopy and antimicrobial activity of copper (ii) complex of furfuraldehyde-2-salisaldehyde thiosemicarbazide1-(2-ydroxybenzylidene)-4-((4hpyran-2yl) methylene) thiosemicarbazide," *Int. J. Recent Trends Sci. And Technol.*, vol. 10, no. 3, pp. 423–429, 2014. [Online]. Available: https://statperson.com/Journal/ScienceAndTechnology/Article/Volume10Issue3/10_3_5.pdf.

[11] K. Bhatt, "Synthesis, characterization and biological screening of schiff bases derived from 4, 6-difluoro-2-amino benzothiazole," *Med. Anal. Chem. Int. J.*, vol. 4, no. 1, pp. 1–7, 2020. DOI: 10.23880/macij-6000157.

[12] Y. Jamil, F. Al-Azab, N. Al-Selwi, T. Alorini, and A. Al-Hakimi, "Preparation, physicochemical characterization, molecular docking and biological activity of a novel schiff-base and organophosphorus schiff base with some transition metal(ii) ions," *Main Group Chem.*, vol. 22, no. 3, pp. 337–362, 2023. DOI: 10.3233/MGC-20101.

[13] Y. Jamil, F. Al-Azab, and N. Al-Selwi, "Novel organophosphorus schiff base ligands: Synthesis, characterization, ligational aspects, xrtd and biological activity studies," *Ecletica Quimica*, vol. 48, no. 3, pp. 36–53, 2023. DOI: 10.26850/1678-4618eqj.v48.3.2023.p36-53.

[14] Y. Jamil *et al.*, "Synthesis, spectroscopic and antibacterial studies of new schiff-base and organophosphrous schiff-base with some transition metal (ii) ions," *J. Qassim Univ. for Sci.*, vol. 1, no. 1, pp. 129–153, 2022. [Online]. Available: https://jnsm.qu.edu.sa/index.php/jnm/article/download/2368/2388.

[15] Y. Jamil, F. Al-Azab, and N. Al-Selwi, "Larvicidal effects of new organophosphorus schiff base compounds against dengue fever vector aedes aegypti (diptera; culicidae)," *Sana'a Univ. J. Appl. Sci. Technol.*, vol. 1, no. 1, pp. 78–87, 2023. DOI: 10.59628/jast.v1i1.156.

[16] A. Musa, J. Na'aliya, and S. Yusuf, "Synthesis, characterization and antimicrobial studies of co(ii), ni(ii), cu(ii) and zn(ii) complexes of a schiff base derived from 3-nitrobenzaldehyde with arginine," *UMYU J. Pure Ind. Chem. Res.*, vol. 2, no. 1, pp. 159–176, 2022. DOI: 10.55688/ujpicr21.017.

[17] M. Hasan, H. Rahman, M. Haque, and M. Islam, "Oxo vanadium (iv) complexes of -amino acid schiff bases and poly pyridyl ligands: Synthesis, characterization and antimicrobial activity," *Asian J. Chem. Sci.*, vol. 14, no. 2, pp. 7–20, 2024. DOI: 10.9734/ajocs/2024/v14i2290.

[18] A. Kamalı, R. Çakmak, and M. Boğa, "Anticholinesterase and antioxidant activities of novel heterocyclic schiff base derivatives containing an aryl sulfonate moiety," *J. Chin. Chem. Soc.*, vol. 69, pp. 731–743, 2022. DOI: 10.1002/jccs.202100511. [Online]. Available: https://onlinelibrary.wiley.com/doi/abs/10.1002/jccs.202100511.

[19] A. Hamad *et al.*, "Schiff bases of sulphonamides as a new class of antifungal agent against multidrug-resistant candida auris," *Microbiol. Open*, vol. 10, p. 1218, 2021. DOI: 10.1002/mbo3.1218. [Online]. Available: https://onlinelibrary.wiley.com/doi/abs/10.1002/mbo3.1218.

[20] B. Shah, V. Kakumanu, and A. Bansal, "Analytical techniques for quantification of amorphous/crystalline phases in pharmaceutical solids," *J Pharm Sci*, vol. 95, no. 8, pp. 1641–1665, 2006. DOI: 10.1002/jps.20644.

[21] A. Patterson, "The scherrer formula for x-ray particle size determination," *Phys. Rev.*, vol. 56, p. 978, 1939. DOI: 10.1103/PhysRev.56.978.

[22] J. Yoe and A. Jones, "Colorimetric determination of iron with disodium-1,2-dihydroxybenzene-3,5-disulfonate," *Ind. Eng. Chem., Anal. Ed.*, vol. 16, no. 2, pp. 111–115, 1944. DOI: 10.1021/i560126a015. [Online]. Available: https://pubs.acs.org/doi/abs/10.1021/i560126a015.

[23] B. Ericsson, T. G., and W. K., "The paper disc method for determination of bacterial sensitivity to antibiotics: Relationship between the diameter of the zone of inhibition and the minimum inhibitory concentration," *Scand. J. Clin. Lab. Investig.*, vol. 12, no. 4, pp. 414–422, 1960. DOI: 10.3109/00365516009065406.

[24] Y. Jamil, F. Al-Azab, N. Al-Selwi, and A. AL-Ryami, “Preparation, characterization, and biological activities of mixed chloroquine and ketoprofen as metal-drug complexes,” *Sana’a Univ. J. Appl. Sci. Technol.*, vol. 2, no. 1, pp. 53–64, 2024. [Online]. Available: http://dx.doi.org/10.59628/jast.v2i1.801.

[25] W. Person, “A criterion for reliability of formation constants of weak complexes,” *J. Am. Chem. Soc.*, vol. 87, no. 2, pp. 167–170, 1965. DOI: 10.1021/ja01080a006.

[26] M. Abdul Galil, A. Al-Hakimi, R. Alshwafy, R. Al Okab, and A. Mutir, “Synthesis, structural studies and microbial evaluation of cu(ii), mn(ii) ni(ii), zn(ii), fe(iii), ru(iii), vo(ii), uo2(ii) complexes of tetradentate oxime-hydrazon ligand,” *Chem. J.*, vol. 1, no. 3, pp. 95–102, 2015.

[27] M. Shakdofa, A. Al-Hakimi, F. Elsaied, S. Alasbahi, and A. Alkwlini, “Synthesis, characterization and bioactivity zn2+, cu2+, ni2+, co2+, mn2+, fe3+, ru3+, vo2+, and uo2+ complexes of 2-hydroxy-5-((4-nitrophenyl) diazenyl)benzylidene)-2-(ptolylamino) acetohydrazide,” *Bull. Chem. Soc. Ethiop.*, vol. 31, no. 1, pp. 75–91, 2017. DOI: 10.4314/bcse.v31i1.7.

[28] A. Raymond *et al.*, “Combined protein construct and synthetic gene engineering for heterologous protein expression and crystallization using gene composer,” *BMC Biotechnol.*, vol. 9, no. 1, pp. 1–15, 2009. DOI: 10.1186/1472-6750-9-37.

[29] Y. Jamil, A. Al-Maqtari, and M. Al-Qadasi, “Ligational and spectroscopic studies on some sulfamethoxazole metal complexes as antimicrobial agents,” *Eur. J. Pharm. Med. Res.*, vol. 4, no. 07, pp. 95–105, 2017. [Online]. Available: https://storage.googleapis.com/journal-uploads/ejpmr/article_issue/1498810674.pdf.

[30] J. Lu *et al.*, “Structures of kibdelomycin bound to staphylococcus aureus gyrb and pare showed a novel u-shaped binding mode,” *ACS Chem. Biol.*, vol. 9, no. 9, pp. 2023–2031, 2014. DOI: 10.1021/cb5001197.

[31] D. Boverhof *et al.*, “Comparative assessment of nanomaterial definitions and safety evaluation considerations,” *Regul. Toxicol. Pharmacol.*, vol. 73, no. 1, pp. 137–150, 2015. DOI: 10.1016/j.yrtph.2015.06.001.

[32] F. Al-Yusufy, M. Al-Qadasy, Y. Jamil, H. Al-Maydama, and M. Akeel, “A comparative study of schiff base chelating resins: Synthesis, uptake of heavy metal ions, and thermal studies,” *Ecletica Quimica*, vol. 43, no. 2, pp. 10–22, 2018. DOI: 10.26850/1678-4618eqj.v43.2.2018.p10-22.